

## Optimization of the priming procedure for Thermally Stimulated Currents with heavily irradiated silicon detectors

---

### **Mara Bruzzi<sup>1</sup>**

*INFN – Firenze, Via G. Sansone, 1, Sesto Fiorentino, Firenze, Italy  
Dipartimento di Energetica, Università di Firenze, Via S. Marta 3, 50139 Firenze  
E-mail: Mara.Bruzzi@unifi.it*

### **Riccardo Mori**

*INFN – Firenze, Via G. Sansone, 1, Sesto Fiorentino, Firenze, Italy  
Dipartimento di Elettronica e Telecomunicazioni, Università di Firenze Via S. Marta 3, 50139 Firenze*

### **Monica Scaringella**

*INFN – Firenze, Via G. Sansone, 1, Sesto Fiorentino, Firenze, Italy  
Dipartimento di Energetica, Università di Firenze, Via S. Marta 3, 50139 Firenze*

### **David Menichelli**

*INFN – Firenze, Via G. Sansone, 1, Sesto Fiorentino, Firenze, Italy  
Dipartimento di Energetica, Università di Firenze, Via S. Marta 3, 50139 Firenze*

We report on the investigation of the radiation damage induced by neutron irradiation on both n- and p-type Magnetic Czochralski silicon pad detectors by the Thermally Stimulated Currents (TSC) technique. Detectors have been irradiated with fast neutrons in the range  $10^{14}$ - $10^{16}$  n/cm<sup>2</sup>. Priming conditions have been studied in detail in order to investigate the residual electric field due to frozen charged traps after the priming step and its influence on the TSC emission. Zero bias TSC measurements have also been performed as an additional tool to study the defects distribution and the residual electric field. The electric field distribution inside the sample and its effect on the TSC emission are qualitatively explained by a band diagrams description.

*9<sup>th</sup> International Conference on Large Scale Applications and Radiation Hardness of Semiconductor Detectors-Rd09  
Florence, Italy  
30 September - 2 October 2009*

---

<sup>1</sup> Speaker

## 1. Introduction

Experiments projected to run at the LHC are designed to have a central tracking detector around the collision region, where high spatial precision and time resolution will be achieved using pixel and microstrip silicon detectors. Such detectors have been manufactured to withstand the surrounding hostile radiation environment: hadron fluences up to  $10^{14}$ - $10^{15}$   $n_{eq}/cm^2$  (1MeV neutron equivalent) will be achieved after ten years operation. An increase of luminosity of the machine (Super-LHC), planned in near future [1], will push hadron fluences values in the inner tracker further up, to values of  $10^{15}$ - $10^{16}$   $n_{eq}/cm^2$ . A detailed radiation damage study on silicon is ongoing to face this extremely severe radiation environment: strong efforts are spent by the scientific community, in particular by the CERN RD50 Collaboration [2], to correlate changes in the electrical properties of the irradiated detectors with radiation-induced lattice defects in silicon.

Radiation-induced defects are investigated by means of spectroscopic techniques as Thermally Stimulated Currents (TSC) [3] and Deep Level Transient Spectroscopy (DLTS) [4]. These techniques permit to identify the activation energy,  $E_t$ , capture cross section  $\sigma$  and concentration  $N_t$  of the defects responsible of carrier trapping. In particular, TSC is adopted at large fluences, when high concentrations of defects are dominating the initial intentional doping. In fact, a major problem of DLTS applied to heavily irradiated silicon is the flattening of the C-V curves observed at high test signal frequency. In silicon detectors, characterised by a rather high initial resistivity, this effect is typically observed for 1MeV neutron fluences higher than  $10^{12}$   $n_{eq}/cm^2$ , so in general DLTS is limited to the study of the low fluence range [5].

Unfortunately, at large hadron fluences problems are encountered also with TSC. In a standard TSC measurement, the diode is cooled down to, e.g., liquid nitrogen/helium temperature with reverse or null bias applied; then the voltage is reduced to zero or reversed in polarity to forward-bias the device. During this time, the traps in the depletion region that previously were empty get filled with free carriers in the neutral bulk. Alternatively, the sample is illuminated with an optical source. A subsequent heating with linear ramp of the reverse-biased sample will cause a peak in current, due to the release of the carriers from the traps. The current peak integrated as a function of time will give the charge released by each trap. Knowing the depletion depth corresponding to the reverse bias applied to the sample, the trap concentration can be derived. The current peak related to the trap should be directly proportional to the depletion depth and thus increase with the applied reverse voltage. Moreover, a saturation of the current peak should occur at full depletion, when the depletion depth equals or overcomes the sample thickness [5]. Nevertheless, after irradiation with high fluence levels and in the presence of high concentrations of defects, it is sometimes observed a decrease of the TSC peaks when increasing the applied reverse voltage: an example is shown in fig. 1 for a n-on-p Si diode irradiated by 24 GeV protons up to  $4.19 \times 10^{14}$   $p/cm^2$ . The TSC spectra show the peak at 30K, previously identified by some of the authors as a radiation-induced

shallow donor occurring in Magnetic Czochralski Si [6]. This defect is considered as the responsible of the higher radiation hardness of magnetic Czochralski Si n-type, as its creation significantly reduces the type inversion effect observed in n-type FZ Si [7]. In fig. 1, the area of the TSC peak related to this defect is decreasing when the reverse bias is increased, reaching a saturation value lower than the low voltage one. Due to this effect, it is not possible to derive, from a TSC measurement, the correct trap concentration: a parameter which is necessary to quantify the effects of this radiation-induced trap on the degradation of the electrical parameters of the device such as leakage current, charge collection efficiency, full depletion voltage.

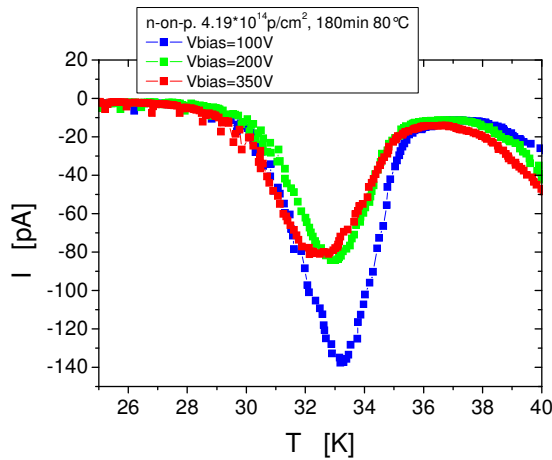


**Figure 1** TSC spectra of the peak at 30K, made with different reverse bias voltages applied to the sample, a n-on-p Si diode irradiated with  $2.5 \cdot 10^{14} n_{eq}/cm^2$ .

In this paper we investigate in detail the TSC methodology in the presence of high concentrations of defects and we demonstrate that the effects mentioned above are due to an inefficient priming of the traps performed before the TSC heating scan. Our study shows how to optimize the priming procedure to evidence the presence of radiation induced defects and then correctly evaluate their concentration. The work is mainly focussed on the TSC peaks occurring in the range 20-80K, as we are interested in getting insights on the behaviour of

the shallow energy levels which can contribute to the effective space charge concentration of the device, as the above mentioned shallow donor at 30K. The second reason is that in the region 20-80K the effect of the leakage current is less important, so we can concentrate our work on the main TSC spectrum features without making a subtraction of the background noise. This latter operation is in fact a significant source of uncertainty in the analysis carried at higher temperatures when heavily irradiated silicon detectors are studied.

## 2. Materials and methods

### 2.1 Devices under test

N- and p-type magnetic Czochralski silicon wafers produced by Okmetic (Finland), <100> orientation and 280 $\mu$ m thickness have been used. On n-type Si with 900  $\Omega$ cm resistivity, p-on-n planar diodes were manufactured (active area 5x5mm<sup>2</sup>) by the WODEAN project of the RD50 CERN Collaboration. These devices were irradiated with reactor neutrons at the Jozef Stefan Institute, Ljubljana, with three fluence values:  $10^{13}$ - $10^{14}$ - $10^{15} n_{eq}/cm^2$ . Annealing of the devices was approximately 1 year at room temperature. On p-type Si with 2k $\Omega$ cm resistivity, n-on-p square diodes with 2.67x2.67mm<sup>2</sup> were produced by the SMART project of the 5<sup>th</sup> INFN

Commission. The devices were irradiated with reactor neutrons at the Jozef Stefan Institute, Ljubljana with fluence in the range  $10^{14}$ - $10^{16}$  n<sub>eq</sub>/cm<sup>2</sup>. Annealing before measurement was corresponding to a few days at room temperature unless differently indicated.

## 2.2 Experimental techniques

Thermally Stimulated Currents were performed on Liquid He vapours, to ensure stable temperatures down to 4.2K, minimize thermal inertia and reduce possible mismatch between the sample and the thermometer. We remind with a sketch (fig. 2) the basic principles of operation of the TSC technique. The priming procedure can be made by current injection or by illumination. In the first case a standard measurement is

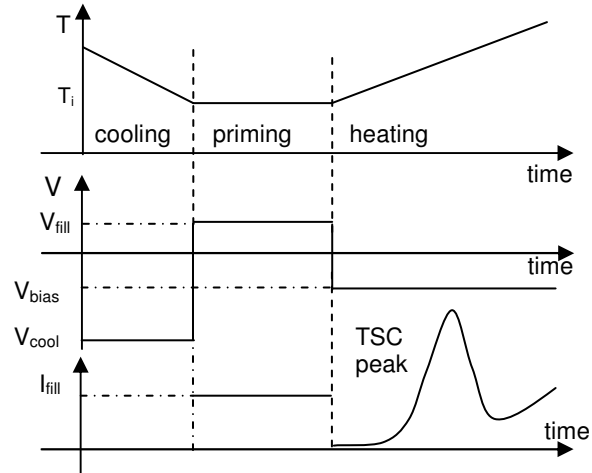


Figure 2 Schematics of a standard Thermally Stimulated Current procedure.

composed by the following steps: (a) cooling with an applied bias  $V_{cool}$ ; (b) applying a forward voltage  $V_{fill}$  at the initial temperature  $T_i$  for a chosen time  $t_{fill}$ , (c) after having applied a reverse bias ( $V_{bias}$ ), temperature is increased linearly and Thermally Stimulated Current is monitored. In the case of priming by radiation the priming step is done by illuminating with a monochromatic electromagnetic source with an applied voltage  $V_{fill}$ .

Priming at  $T_i$  (step (b)) provides an injection of carriers which are trapped by the energy levels associated to the radiation induced defects: a current  $I_{fill}$  will flow through the sample. Trapping occurs within the bulk according to the asymmetrical potential distribution induced by the external polarization ( $V_{bias}$ ). If after priming electrodes are short-circuited ( $V_{bias}=0$  at step (c)) the carriers at electrodes and in the bulk redistribute themselves in order to establish zero voltage and zero field boundary conditions. Charges frozen at low temperature bring to a non-uniform electric field. A non-monotonous potential distribution with minima and maxima corresponding to zero electric-field planes (ZFPs) settles [8]. During the heating scan the system is brought back to the fundamental equilibrium state with charges redistributing into the volume and charge injection occurring at the electrodes, giving rise to a current detected in the external circuit, the Zero Bias Thermally Stimulated Current (ZB-TSC). Charge relaxation during the heating scan of the ZB-TSC can be discussed [9] in terms of motion of the zero electric-field planes (ZFP) along the sample depth. Details on the ZB-TSC technique applied on different semiconductor materials are reported in [10,11].

### 3. Experimental results

A set of TSC and ZB-TSC measurements on p-on-n and n-on-p Si devices irradiated in the range  $10^{14}$ - $10^{16}$   $n_{eq}/cm^2$  are presented here. Current priming and optical priming are investigated separately. In the next section we will show how, from these measurements, we can get important information about the electric field distribution into the irradiated sample and thus explain the experimental results shown in this section.

#### 3.1 Current priming

Figure 3 shows two TSC measurements made on n-on-p Si irradiated up to  $10^{15}$   $n_{eq}/cm^2$  after current priming with same  $V_{cool}$  and  $V_{bias}$  and different  $V_{fill}$ . A larger  $V_{fill}$  brings to an increase of  $I_{fill}$  and thus higher TSC peaks, as expected: increasing  $I_{fill}$  more charges are trapped at defects, so TSC emissions is higher.

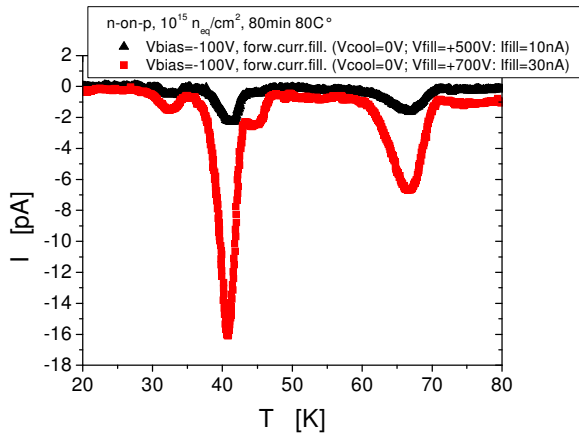


**Figure 3** TSC on n-on-p Si sample irradiated up to  $10^{15}$   $n_{eq}/cm^2$ , annealed 80min at  $80^\circ C$ , with different  $V_{fill}$ .

as expected: increasing  $I_{fill}$  more charges are trapped at defects, so TSC emissions is higher.

Figure 4 (a) shows a set of ZB-TSC performed on a n-on-p diode irradiated with  $10^{14}$   $n_{eq}/cm^2$  with different  $V_{cool}$ , zero  $V_{bias}$  and  $V_{fill}$ . This plot evidences that it is not necessary to have a priming stage to obtain a TSC signal. Cooling under reverse bias builds up a residual field (opposite to the cooling voltage) in the sample, due to the charges frozen in the radiation induced traps. This field increases with  $V_{cool}$  as it can be seen from the initial part of the

emission while it changes together with the relaxation of charge at higher temperatures. In figure 4 (b) we observe what changes in a ZB-TSC when applying a  $V_{fill}$ :  $I_{fill}$  decreases when  $|V_{cool}|$  increases.

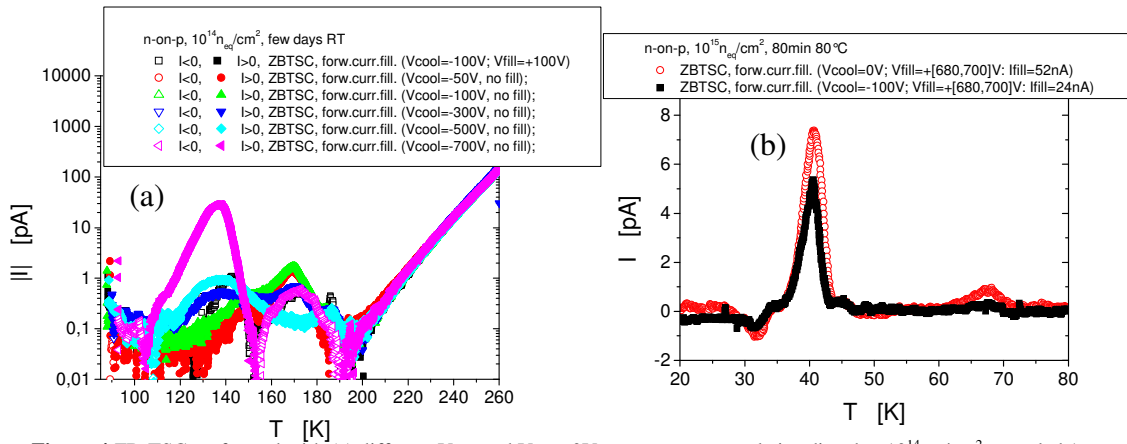


**Figure 4** ZB-TSC performed with (a) different  $V_{cool}$  and  $V_{fill} = 0V$ , on a n-on-p sample irradiated at  $10^{14}n_{eq}/cm^2$  annealed 1 year at RT ; (b) different  $V_{cool}$  and  $V_{fill} = +[680,700]V$ , on a n.on.p sample irradiate at  $10^{15}n_{eq}/cm^2$ , annealed 80min at 80°C.

### 3.2 Optical priming

Optical priming is performed with an infrared source with energy above gap. Assuming that the excitation is uniform in the sample volume, the charge distribution is independent on the residual one, so that the influence of the cooling voltage can be neglected. Figures 5 (a) and (b) show the dependence of TSC/ZB-TSC peak heights on the bias applied during illumination,  $V_{fill}$ . In both measurements, we observe that a reverse  $V_{fill}$  gives lower TSC peaks and higher ZB-TSC emissions with respect to a forward voltage  $V_{fill}$ .

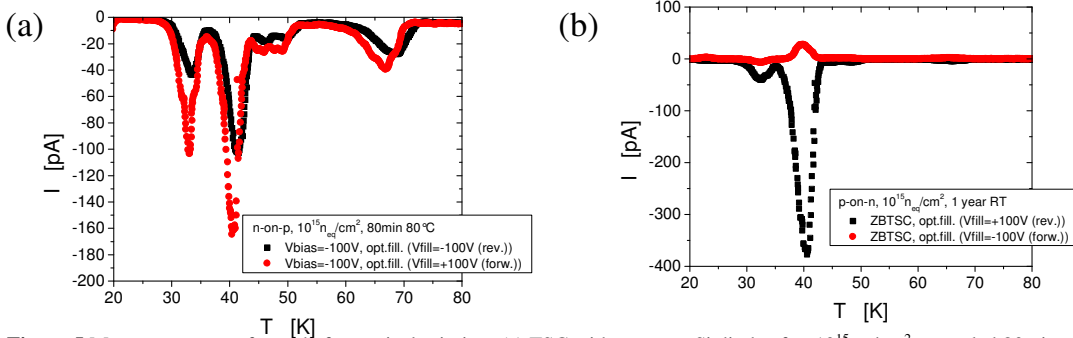


**Figure 5:**Measurements performed after optical priming: (a) TSC with a n-on-p Si diode after  $10^{15}n_{eq}/cm^2$ , annealed 80min at 80°C, with same  $V_{bias}$  and different  $V_{fill}$ ; (b) ZB-TSC p-on-n Si diode after  $10^{15}n_{eq}/cm^2$ , annealed 1 year at RT, with different  $V_{fill}$ .

Figure 6 shows the comparison of the forward current and the optical priming, in TSC at 200V on n-on-p sample irradiated at  $10^{15}n_{eq}/cm^2$  (cooling in reverse at 100V and forward filling at 700V; illumination with reverse  $V_{fill}$  100V). It can be seen that illumination gives a more efficient priming than forward current filling, even when the former is not optimally performed (reverse  $V_{fill}$ ).

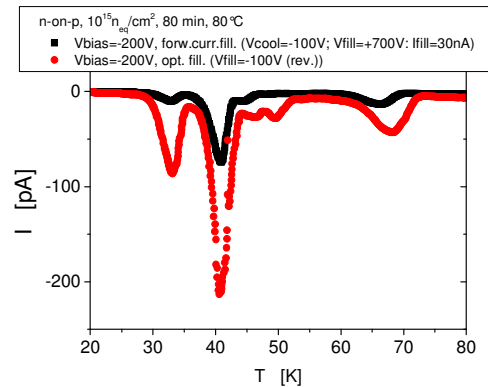


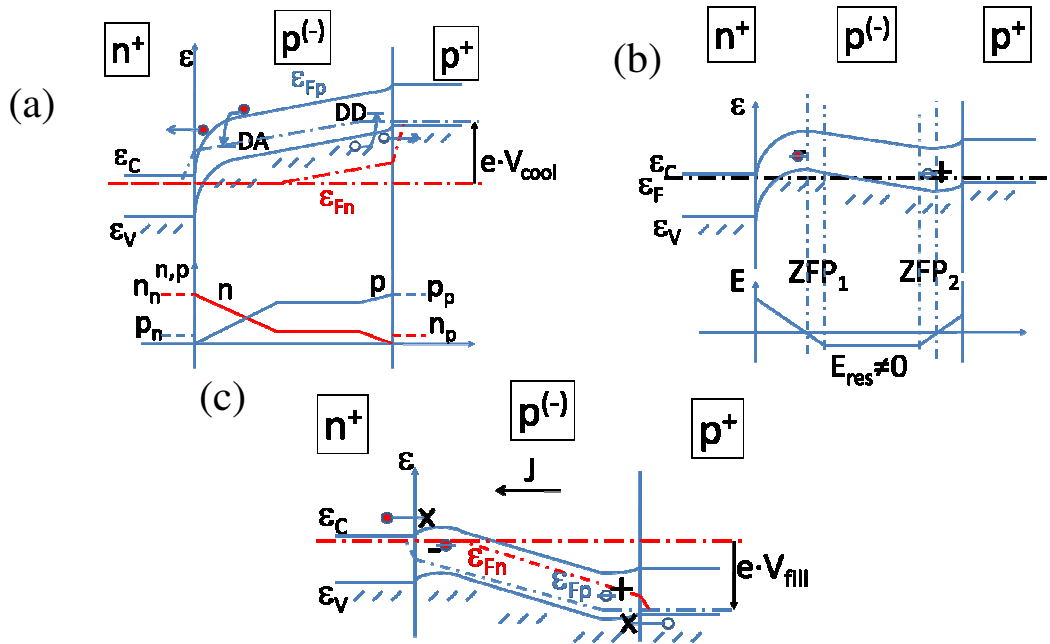
**Figure 6** Comparison of TSC with forward current and optical filling (n-on-p Si  $10^{15}n_{eq}/cm^2$ , 80min at 80°C).

### 3.3 Discussion

The experimental results shown in the previous section are a selection of a vast amount of TSC data obtained performing different priming procedures on different samples and irradiation conditions. The data show the dependences of TSC/ZB-TSC emissions on the priming parameters, summarized as follows:

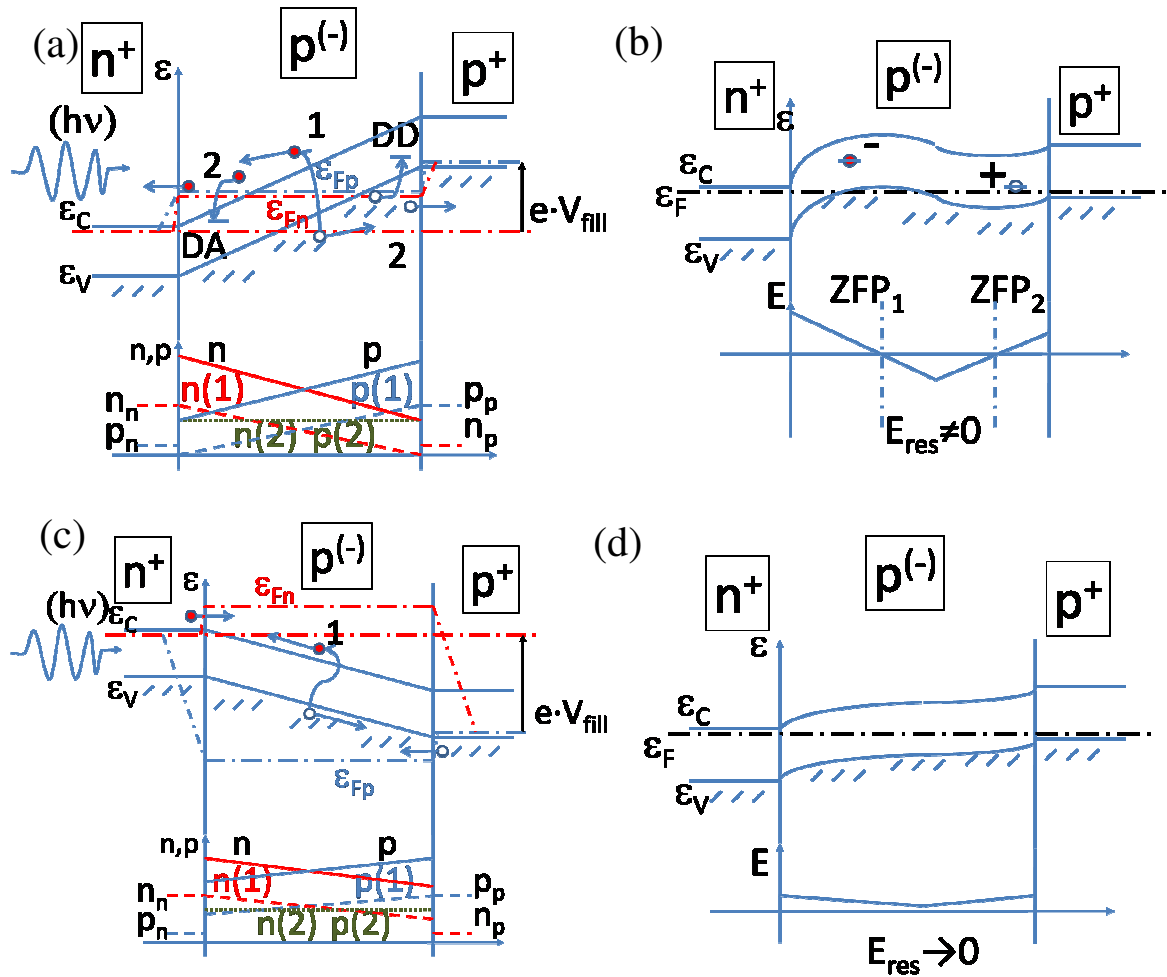
- (a) the TSC peak height increases with the filling current as a higher current drives more carriers which are trapped at the defects, the ZB-TSC peak height depends on both the filling current and the residual electric field established during the cooling procedure;
- (b) the TSC peak height is higher, ZB-TSC is lower, after cooling and filling with the illumination in forward voltage, as this allows one to get higher filling current but lower residual field;
- (c) the cooling bias provokes a residual electric field within the device, due to charge frozen at defects within the depleted region; this residual field is opposed to the one externally applied, so it generally tends to decrease the TSC emission while it is completely responsible of the ZB-TSC;
- (d) forward current filling is less efficient for higher cooling voltage as the filling current decreases with the reverse voltage amplitude; this means that the residual electric field is opposing the priming process;
- (e) optical filling is more effective than forward current filling as it enhances the current flowing (also at the lowest temperature and independently on the residual charge distribution, unlikely the forward current filling).

To put into a organic view all these experimental evidences a model has been developed by us, in terms of band bending changes within the sample thickness during the TSC and ZB-TSC steps. Fig. 7 shows the band diagram of a heavily irradiated n-on-p Si diode during various steps of a TSC/ZB-TSC measurement when current filling is carried out. Fig. 7 (a) sketches the band diagram and the free carriers distribution along the sample thickness when the sample is cooled down with an applied reverse bias. Free electrons and holes are trapped asymmetrically accordingly to the potential distribution due to the externally applied polarization  $V_{cool}$ . Two main defects are shown: a deep acceptor DA, capturing electrons at the  $n^+$  electrode and a deep donor DD capturing holes in the proximity of the  $p^+$  electrode. Fig. 7 (b) depicts the band diagram afterwards, when the bias is switched to zero. The residual electric field distribution shown below is due to the charges frozen in defects during the cooling stages.  $ZFP_1$  and  $ZFP_2$  are the zero-field planes, corresponding to points of zero electric field in the sample. Fig. 7 (c) shows the band diagram during the filling stage made by applying a forward  $V_{fill}$  to the sample, to inject a forward current in the device. The band bending at the electrodes, due to the residual electric field created in the cooling stage, is now behaving as a potential barrier preventing the injection of majority carriers into the bulk: electrons from the  $n^+$  side and holes from the  $p^+$  side. This potential barrier makes the priming stage quite inefficient: a lower filling current will flow into the sample.



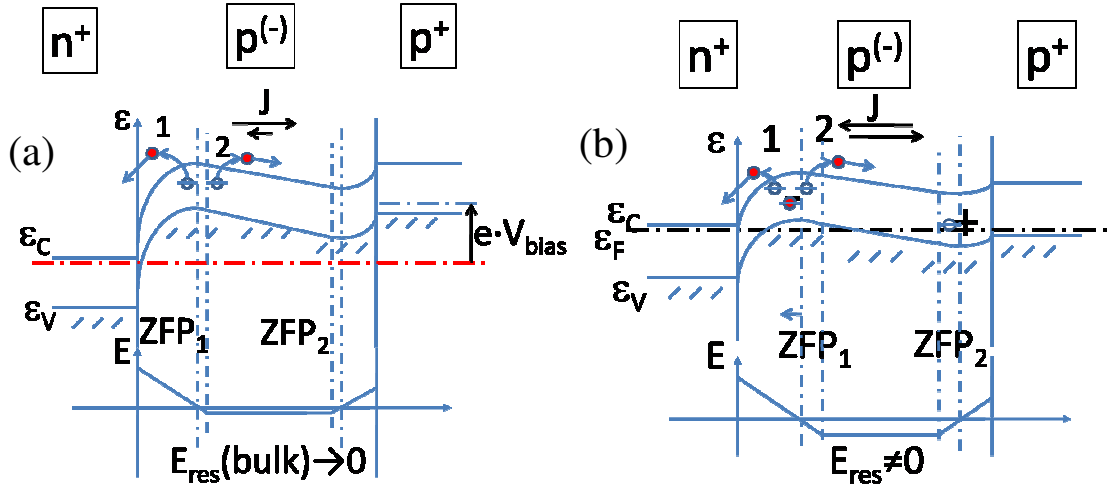
**Figure 7** Band diagram of the irradiated n-on-p Si diode during forward current priming. (a) cooling with an applied reverse bias; (b) band diagram and electric field distribution at null bias after cooling, when charge is frozen in defects; (c) band diagram during the current filling stage.

Fig. 8, shows the band diagram of a heavily irradiated n-on-p Si diode in case an optical filling is carried out. The potential energy distribution is determined by the bias voltage acting on the sample without residual field contribution. The free carrier concentrations result from the optical illumination (which, we assume, generates free carriers uniformly in the material) and are distributed accordingly to the potential distribution determined by the filling voltage. Fig. 8 (a) sketches the band diagram and the free carriers distribution when the sample is optically primed with an applied reverse bias. Electrons and holes are trapped in the depleted regions close to the electrodes by the deep donors and acceptors respectively. While the free carrier concentrations generated by the optical priming,  $n(1)$  and  $p(1)$  are almost uniform, the effect of the applied reverse voltage is to distribute the carriers asymmetrically giving the contributions  $n(2)$  and  $p(2)$ : as a result the total free carriers concentrations  $n$  and  $p$  are asymmetric. Fig. 8 (b) describes the metastable condition afterwards, when the bias is switched to zero, before the heating scan. The band diagram and the relative residual electric field distribution, due to the charges frozen in defects during the optical priming stage, are shown. Fig. 8 (c) shows the band diagram and the free carriers distribution during the optical priming performed with a forward voltage  $V_{fill}$  applied to the sample. In these conditions, the resulting free carrier concentrations are generated and distributed almost uniformly, and so is the trapping of carriers at deep acceptors and donors. The band bending in the metastable condition afterwards is not suffering of the presence of the residual field (figure 8 (d)).



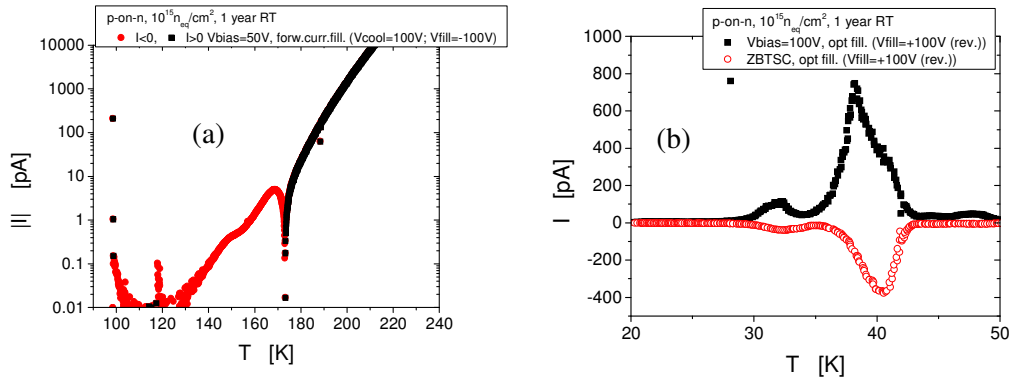
**Figure 8** Band diagrams and free carriers concentrations of the irradiated n-on-p Si diode during optical priming with reverse  $V_{fill}$  (a) and forward  $V_{fill}$  (c). Band diagrams and electric field distributions in the metastable condition after the priming stage in the case of reverse  $V_{fill}$  (b) and forward  $V_{fill}$  (d). Herein are indicated the processes of free carrier generation due to optical excitation (1) and trapping (2).

Fig. 9 describes band bending and electric field distribution during the TSC and ZB-TSC heating scans. It is referred to forward current priming conditions, and for simplicity, only electron emission is shown. The drift current signal originated by carrier emission can have either positive or negative sign, depending on where carriers are emitted. Carriers emitted by traps in a region where the electric field is positive will give rise to a positive current (1), whereas if the electric field is negative the current sign will be negative (2). The effect is complicated by the fact that charge is redistributed into the volume and the Zero Field Planes move during the heating scan, so the regions where the electric field have a different sign is changing during the measurement. The priming leaves a metastable condition where only a portion of the volume is filled; moreover the opposite electric field will give rise to an opposite current component that will reduce the positive current signal.



**Figure 9** (a) Band diagram and electric field distribution during a TSC, measured with a reverse bias applied to the sample; (b) band diagram and electric field distribution during a ZB-TSC, when no bias is applied to the sample. Herein are indicated the components of the electron current in the contact (1) and in the bulk (2) regions.

In a TSC measurement the component due to the residual field is opposite to the external and the built-in components. In general, in a TSC the external field component dominates so that the current is always of the same sign of the externally applied voltage. Nevertheless, for heavily irradiated silicon diodes, the situation can be reversed: the residual electric field in the bulk can be so high to dominate the current emission also in TSC.



**Figure 11** (a) TSC measurement performed after cooling with a reverse bias of 100V, current priming with a forward voltage of 100V, and measuring the TSC with an applied reverse bias of 50V. The negative current observed in the range 100-170K is due to the residual electric field within the silicon bulk. (b) TSC (black squares) and ZB-TSC (red circles) measurements performed on p-on-n sample irradiated at  $10^{15} \text{ n}_{\text{eq}}/\text{cm}^2$  after optical priming at reverse  $V_{\text{bias}} = 100\text{V}$ .

As an example a TSC measurement performed on a p-on-n Si diode irradiated with  $10^{15} \text{ n}_{\text{eq}}/\text{cm}^2$  with  $V_{\text{cool}}=100\text{V}$ ,  $V_{\text{fill}}=-100\text{V}$  and  $V_{\text{bias}}=50\text{V}$  is shown in fig. 11 (a). In the temperature range up to 175K the measured current is negative although a positive bias voltage is applied, for higher temperatures the current becomes positive indicating a relaxation of the residual field. As another example in fig. 11 (b) we show together TSC and ZB-TSC measurements in the lower temperature range, performed after an illumination priming in reverse filling voltage on the p-on-n Si diode irradiated with  $10^{15} \text{ n}_{\text{eq}}/\text{cm}^2$ . The discontinuity in

the TSC spectrum corresponds to an increase of the ZB-TSC, and the signal appear distorted respect to the typical TSC emission curve in the range of the ZB-TSC peak. The ZB-TSC emission reveals that at such temperature range, the residual charge in the bulk dominates.

Finally, it is observed that when performing TSC measurements with the same priming, the resulting charge distribution frozen being the same (however it is subtotal or total), the TSC peak increases with the bias voltage. Fig. 12 shows the TSC measurements performed at 100V and 200V, after the same priming by cooling at null bias and forward current filling at about 30nA.

#### 4. Conclusions

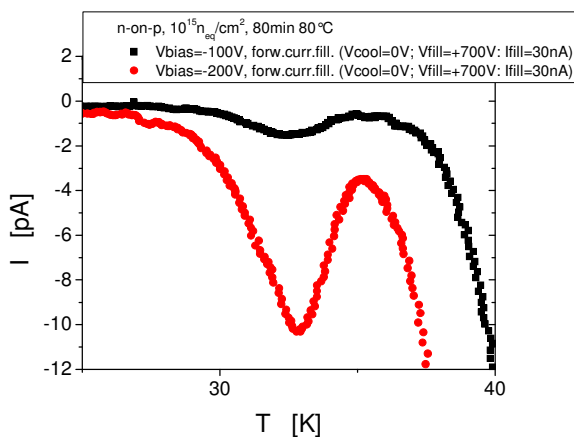


**Figure 12** TSC measurements performed on n-on-p sample irradiated at  $10^{15} n_{eq}/cm^2$ , annealed 80 min at  $80^\circ C$ , at 100V and 200V, after cooling at null bias and forward filling with 700V (30nA).

TSC and ZB-TSC analyses were carried out to inspect radiation-induced defects in both p- and n-type MCz Si pad detectors after irradiation with reactor neutrons in the range  $10^{14}$ - $10^{16} n_{eq}/cm^2$ . Priming procedures have been investigated to optimize the visualization of traps by TSC, in particular in the range 20-80K, typical of radiation-induced shallow traps. A band diagram model has been developed to describe the various features observed experimentally by changing the operative parameters in the TSC/ZB-TSC scans. The analysis allowed us also to inspect the electric field distribution within the irradiated device and get evidence of the presence of a residual electric field due to charges frozen at traps in bulk and barriers close to the electrodes. Residual electric field in the bulk can be so high, in highly irradiated device, to dominate the current emission both in TSC and ZB-TSC. Our study allowed us to optimize the best priming procedure for TSC to get a correct trap concentration of the radiation-induced defects: optical filling with an infrared source, performed with an applied forward bias. The application of the forward voltage in fact avoids the formation of the residual electric field opposing to the injection of majority carriers during priming and allows the inspection of the whole active volume of the sample. Moreover, in case of optical filling with an applied forward bias the cooling voltage adopted has no influence on the priming.

It is important to note that our study gives evidence of a significant electrical polarization of heavily irradiated Si diodes when they are reverse biased and kept at low temperature, which is a typical operative condition of any microstrip and pixel Si detector in high energy physics experiments. This polarization field could have a significant role in the degradation of important properties as charge collection efficiency of the irradiated devices. We therefore plan in near

future to make use of the band diagram model developed in this study to investigate the charge collection properties of heavily irradiated silicon detectors kept in reverse-bias and low-temperature operative conditions.

### Acknowledgements

Work performed in the framework of the WODEAN project of the CERN RD50 Collaboration and SMART INFN project. Authors would like to thank Eckhart Fretwurst and Donato Creanza for providing the samples and Mrs. Alessandra Giannini for technical assistance.

### References

- [1] F. Gianotti, et al., *Physics potential and experimental challenges of the LHC luminosity upgrade*, hep-ph/0204087, April 2002
- [2] RD50 Collaboration, Status reports, <http://rd50.web.cern.ch/rd50/>.
- [3] H. Schade, D. Herrick, *Determination of deep centers in silicon by thermally stimulated conductivity measurements*, Solid State El., 12 (1969) 857.
- [4] D. V. Lang, Deep-level transient spectroscopy: A new method to characterize traps in semiconductors J. Appl. Phys. 45 (1974) 3023
- [5] P. Blood and J.W. Orton. The *Electrical Characterization of Semiconductors: Majority Carriers and Electron States*. N.H. March, Academic Press (1992).
- [6] M. Scaringella et al., *Localized energy levels generated in Magnetic Czochralski silicon by proton irradiation and their influence on the sign of space charge density* Nucl. Instr. Meth. A 570 (2007) 322.
- [7] R. Wunstorf, M. Benkert, N. Claussen, N. Croitoru, E. Fretwurst, G. Lindstroem and T. Schulz, *Results on radiation hardness of silicon detectors up to neutron fluences of  $10^{15}$  n/cm<sup>2</sup>*. Nucl. Instr. and Meth. A, 315 (1992) 149.
- [8] D. Menichelli, R. Mori, M. Scaringella and M. Bruzzi *Zero-bias thermally stimulated currents (ZB-TSC) spectroscopy of deep traps in irradiated silicon particle detectors* Nucl. Instr. Meth. A 612 (2010) 530.
- [9] B. Gross and M.M. Perlman, *Short-circuit currents in charged dielectrics and motion of zero-field planes*, J. Appl. Phys. 43 (1972) 853.
- [10] W.S. Lau, K.F. Wong, T. Han and N. Sandler, *Application of zero-temperature gradient zero-bias thermally stimulated current spectroscopy to ultrathin high-dielectric-constant insulator film characterization*, Appl. Phys. Lett. 88 (2006) 172906
- [11] W.S. Lau, T.C. Chong, L.S. Tan, C.H. Goo, K.S. Goh and K.M. Lee, *Study of electron traps in semi-insulating gallium-arsenide buffer layers for the suppression of backgating by the zero-bias thermally stimulated current technique*, Appl. Phys. Lett. 61 (1992) 49.